RSC Advances

PAPER

View Article Online
View Journal | View Issue

Cite this: *RSC Adv.*, 2015, **5**, 23778

Mechanistic approach on heat induced growth of anionic surfactants: a clouding phenomenon†

Arti Bhadoria,[a] Sugam Kumar,[b] Vinod K. Aswal[b] and Sanjeev Kumar‡*[a]

Different anionic surfactants: tetra-*n*-butylammonium dodecylsulphate (TBADS), tetra-*n*-butylammonium-α-sulfonato myristic acid methyl ester (TBAMES) and tetra-*n*-butylphosphonium dodecylsulphate (TBPDS) were synthesized. Though all the surfactants are ionic in nature, they show the clouding phenomenon on heating. The effect of temperature on the solution behaviour (micellization and clouding) of the synthesized surfactants was studied by conductometry, dynamic light scattering (DLS), nuclear magnetic resonance (NMR), small angle neutron scattering (SANS) and polarising optical microscopy (POM) studies. The experimental cmc data of TBADS exhibits a U-shaped curve when plotted against temperature. Conductivity measurements follow different trends with temperature for various fixed concentrations of TBADS. Conductivity increases with temperature at lower TBADS concentrations, while an unusual decrease was observed with temperature for higher TBADS concentrations. NMR data with temperature also show peculiarity similar to that observed conductometrically. The broadening and splitting of the NMR peaks with increasing temperature is in agreement with the growth of micelles and formation of two morphologies. The grown aggregates tend to exhibit a stronger attractive potential relative to individual spherical micelles. The increase in δ (ppm) values along with the broadening of the peaks in the NMR spectra on increasing temperature corroborates the dehydration of the counterion and the increase in attractive forces among the grown aggregates. This proposition has been supported by the DLS and SANS results. It is experimentally confirmed that the formation of bigger aggregates through the fusion of grown micelles, which is facilitated by the dehydrated counterion on increasing the temperature and the onset of attractive interactions, is the key process involved in the clouding phenomenon of ionic surfactant solutions. The Langer-Schwartz's nucleation theory and the growth of micelles beyond the critical droplet size, resulting in a phase separation, are confirmed through the POM results. Thus, the solution response complements with both conventional ionic and nonionic surfactants, depending upon the concentration/temperature. This added feature can be due to the substitution of Na^+ by a quaternary counterion in a typical anionic surfactant.

Received 19th January 2015
Accepted 16th February 2015

DOI: 10.1039/c5ra01090j

www.rsc.org/advances

Introduction

The interfacial water in the immediate vicinity of the hydrophobic and hydrophilic surfaces of an amphiphile plays a predominant role in various phenomena.[1,2] Therefore, the knowledge of the factors that affect aggregate formation becomes important in the physical synthesis of self assemblies. It has been well understood that water molecules confined in various micro-heterogeneous nano confinements (such as micelles, reverse micelles, liposome, and lamellae) behave in a markedly different manner compared to bulk water. The property of the confined water is dependent upon the nature of the surfactant molecule (ionic or nonionic) constituting a self assembly system. Nonionic surfactants are believed to possess aqueous solubility due to hydrogen bonding between water and surfactant molecules, which breaks on increasing the temperature, resulting in a cloudy or turbid solution. This particular temperature is called the cloud point (CP).[3,4] The CP is a principal feature of nonionic surfactant solutions, and it is uncommon with ionic surfactants due to the presence of electrostatic repulsions between the charged aggregates. Some ionic surfactants with high salt concentration, surfactants with a large head group or large counter ions and some mixed cationic and anionic surfactant solutions are known to show the clouding phenomenon.[5–10] Most of the studies with

[a]*Soft Material Research Laboratory, Department of Chemistry, The Maharaja Sayajirao University of Baroda, Vadodara 390 002, India. E-mail: drksanjeev@gmail.com*

[b]*Solid State Physics Division, Bhabha Atomic Research Centre, Trombay, Mumbai 400 085, India*

† Electronic supplementary information (ESI) available: Individual NMR spectra, NMR at variable temperatures, 2D NOESY spectra, SANS spectra of various synthesized and some conventional surfactants (Fig. S1–S13) and (Tables T1–T4). See DOI: 10.1039/c5ra01090j

‡ Present address: Department of Applied Chemistry, The Maharaja Sayajirao University of Baroda, Vadodara 390 002, India.

conventional anionic surfactants are carried out with the TBA^+ counterion added externally or derived from the surfactant (namely, tetra-*n*-butylammonium dodecylsulphate, TBADS) itself.[8,11–14] Recently, the effects of the addition of quaternary ammonium bromides on the aggregation behaviour/structural transition of a few anionic surfactants have also been studied using various techniques.[15,16] However, the detailed morphological transition caused by heating remains nearly unexplored at the molecular level. A fair discussion regarding the morphological aspects for the clouding phenomenon of nonionic surfactants can be found in a recent review.[10] However, very little is known regarding the morphologies present in ionic surfactant solutions below and at/above the CP. Different types of assemblies can be transformed in response to variations in environmental factors. Temperature plays an important role in such transitions.[17,18] Usually, on increasing the temperature, the transition from a higher order aggregate to a lower order state takes place.[19–21] Among the ionic surfactants, micellar growth behaviour on heating is common only for some cationic surfactants mixed with oppositely charged surfactant/hydrotropes.[17,22,23] However, to date, studies on temperature induced micellar growth are rare for single anionic surfactant systems. Therefore, some key questions need to be addressed to understand the rationale behind their morphology and solution behaviour. Different models, such as the onset of attractive interactions, multiple bridging among the ionic micelles through the alkyl tails of their counterion, formation of the connected micellar network or strongly orientation dependent interactions between water and micellar head groups, without any experimental evidence, have been employed to provide the mechanism for the clouding phenomenon.[14,24–28] However, most of the time the discussion regarding the mechanism of the clouding phenomenon in charged micellar solutions ended with a hazy picture.[5,8,24,29–34] Here, an attempt has been made to rationalize the observations and provide experimental evidence along with qualitative arguments regarding the solution behaviour of typical anionic surfactants and the morphological transitions involved therein, below and above the CP using various physicochemical techniques. Therefore, different anionic surfactants having quaternary counterions, *i.e.*, tetra-*n*-butylammonium dodecylsulphate (TBADS) tetra-*n*-butylammonium-α-sulfonato myristic acid methyl ester (TBAMES), tetra-*n*-butylphosphonium dodecylsulfate (TBPDS), were synthesized.

Both micelles and grown aggregates coexist at the CP and beyond the CP. A potential application for grown aggregates can be storage or controlled release applications (*e.g.* in cosmetics, drug delivery *etc.*). It has also been reported that the loading of DNA into vesicles can greatly be improved using micrometer-sized vesicles.[35] Clouding at low temperatures and concentrations may find use in cloud point extraction (CPE) systems for the extraction of various charged and thermally labile moieties.

Experimental section

Materials

Sodium dodecylsulphate, SDS (≥99%), tetra-*n*-butylammonium bromide, TBAB, (99%), tetra-*n*-butylphosphonium bromide, TBPB (99%) and Triton X-100 (ultra) were purchased from Sigma, St Louis, USA. α-Sulfonato myristic acid methyl ester (MES), a gift sample (Lion corporation, Tokyo), was recrystallized using dry ethanol before use. The studied anionic surfactants were prepared by mixing equimolar solutions of SDS/MES with TBAB/TBPB. The respective clear mixtures were stirred at room temperature for 62 h. The formed compound was then extracted with dichloromethane, DCM, as the solvent, and finally after vacuum drying, the isolated viscous mass was used for further analysis. The purity of all the surfactants, namely, tetra-*n*-butylammonium dodecylsulphate (TBADS), tetra-*n*-butylammonium-α-sulfonato myristic acid methyl ester (TBAMES) and tetra-*n*-butylphosphonium dodecylsulphate (TBPDS), was confirmed by ^{1}H NMR, IR, mass spectrometry and surface tensiometry. The water used to prepare the aqueous surfactant solutions was double distilled in an all-glass distillation apparatus. The specific conductivity of the water was in the range of 2–4 $\times$ 10^{-6} S cm^{-1}. D_2O used in the sample preparation for NMR was 99.9 atom% D, and was purchased from Sigma-Aldrich, St Louis, USA.

Experiments

Conductometric measurements were carried out using a conductivity meter EUTECH cyberscan CON510 (cell constant 1 cm^{-1}) with an inbuilt temperature sensor. A pre-calibrated conductivity cell was used to obtain specific conductance at an appropriate concentration range. The temperature of the sample solution was precisely controlled by a SCHOTT CT 1650 thermostat with an accuracy of ±0.1 °C. The cell with an appropriate amount of the solvent (water) in a vessel was thermostated for at least 30 minutes prior to the measurement. The conductivity runs were carried out by adding a concentrated surfactant solution to the solvent water. The critical micelle concentration (cmc) and degree of counterion dissociation (α) values for the synthesized anionic surfactants were determined from the intersection point between the two straight lines (in the plot of the [surfactant] *vs.* specific conductance (κ)), and the ratio of the slopes of the postmicellar to that of the premicellar portions of the straight lines.

The CP values were obtained by placing sample tubes containing surfactant solutions with a fixed concentration into a temperature-controlling water bath. The onset of turbidity temperature (visual observation) was noted. The system was allowed to cool, and the temperature at which the disappearance of turbidity took place was also noted. The average of these two temperatures was taken as the cloud point (CP). This procedure was repeated for the same sample and nearly two concurrent values (within ±0.1 °C) were considered as the final CP. Similar CP measurements were made by diluting the samples using double distilled water to collect CP data at various concentrations.

DLS measurements were performed using a Brukhaven 90 plus particle size analyser. A solid laser operated at 660 nm with a maximum power output of 15 mW with the scattering angle of 90° was used. The sample was filtered (0.22 μm) to avoid interference from dust particles. The correlation

functions were analyzed by the method proposed by Contin and Cumulant to have an idea of the mean diameter and polydispersity index.

NMR spectra were obtained with Bruker Avance 400 Spectrometer at different temperatures (20–70 °C). All the surfactant solutions were prepared in D_2O. About 0.6 ml of solution was transferred to a 5 mm NMR tube and chemical shifts were recorded on the δ (ppm) scale.

SANS measurements were carried out using a SANS spectrometer at Dhruva Reactor, Bhabha Atomic Research Centre, Trombay, India.[36] The samples were placed in a quartz sample holder having a thickness of 2 mm and the temperature was varied below and above the CP. The measured SANS data were corrected and normalized to an absolute scale using a standard procedure.[26,37] In SANS measurements, coherent differential scattering cross-section per unit volume ($d\Sigma/d\Omega$) as a function of scattering vector Q ($=4\pi \sin\theta/\lambda$) is measured, where 2θ is the scattering angle, and for a monodisperse micelle solution, it can be expressed as follows:[38]

$$d\Sigma/d\Omega = n_m V_m^2(\rho_m - \rho_s)^2\{\langle F^2(Q)\rangle + \langle F(Q)\rangle^2[S(Q) - 1]\} + B \quad (1)$$

where n_m and V_m are the number density and volume of the micelle, respectively, $F(Q)$ is the single particle form factor that depends on the shape and size of a particle, $S(Q)$ is the interparticle structure factor and B denotes the incoherent scattering background contributed from hydrogen in the micelle. The dimensions (semi major axis (a), semiminor axis ($b = c$)), aggregation number, N ($=4\pi ab^2/3v$, where v is the volume of the surfactant tail) and the average charge of the micelles were determined from this analysis. The relevant expressions used are similar to those reported earlier.[26,27]

To get visual observations, experiments were performed using a Leica DFC 295 optical microscope fitted with Leica (Germany) Lens (4×, 10×, 20× and 50× magnifications). Images were recorded using an inbuilt Leica camera at 20×. The temperature was maintained, using a Linkam heating stage, LST 420, controlled by the Leica application suite computer software, LAS-V41.

Results and discussion

The micellar surface is characterised by the presence of water of hydration. The quaternary counterion TBA^+/TBP^+ (from the surfactant itself), in addition to a positive charge, carries four butyl chains. Therefore, it can interact hydrophobically with the alkyl chains of the surfactant molecules, which constitute the micelle, as well as they can electrostatically interact with oppositely charged micellar head groups. The butyl chains of such counterions can get embedded between the monomers of a micelle due to hydrophobic interactions. Moreover, due to the bulky nature of the counterion, the micellar surface can be quickly saturated with TBA^+/TBP^+ and the remaining counterions may be used to link various micelles together, resulting in bigger aggregates that cause clouding.[8] Micellar parameters[39] and CP data for the synthesized surfactants were acquired by the procedure given in the Experimental section.

Effect of temperature on micellar parameters

To understand the clouding behavior of quaternary counterion surfactants, the cmc data of surfactants that have Na^+ and quaternary counterions were compared. The cmc values are higher for the surfactants that have an inorganic counter ion (*e.g.* Na^+) than the surfactants containing a quaternary organic counter ion, TBA^+ or TBP^+ (Table T1, ESI†). Electrostatic as well as hydrophobic interactions may force the organic counter ion to bind with the micellar surface and initiate the phenomenon of micellization at a lower concentration. However, the cmc value is found to be higher for TBPDS than TBADS. The electrostatic repulsive interaction between similarly charged head groups will also be less depleted with TBP^+ than TBA^+, resulting in higher cmc values for TBPDS.

Further, TBADS is chosen for a detailed micellization study at different temperatures. Fig. 1 shows the plots of κ *vs.* [TBADS] at various temperatures. These plots are used to determine cmc and alpha values at different temperatures, which are summarized in Table 1. Cmc variation with temperature shows a U shaped behavior (Fig. 2a). A detailed discussion on the U shaped behavior of cmc with temperature can be found in an earlier report.[40] However, the temperature of the minimum cmc (T_m) was found to be higher than that reported for conventional ionic surfactants (*e.g.* SDS).[41] The α value shows a gradual decrease with temperature (Fig. 2b). The reported α data on conventional ionic surfactants suggest that α shows a weak dependence on temperature.[42] In another study, an increase in α has also been reported with temperature.[43] The two observations mentioned above (higher T_m and decreasing α) indicate that TBADS responds differently on heating. A similar hint was intimated from the literature by Bales and Zana.[8]

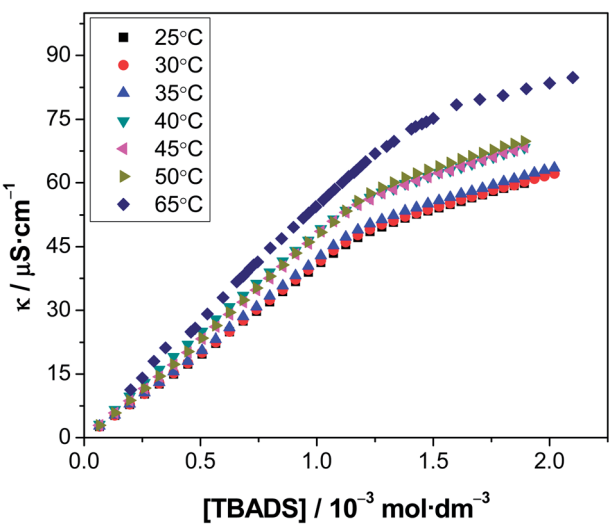

Fig. 1 Variation of specific conductance (κ) *vs.* concentration plots for TBADS at different temperatures.

Table 1 cmc and α values for TBADS at different temperatures

Temperature (°C)	cmc 10^{-3} (M)	α
25	1.22	0.42
30	1.21	0.39
35	1.19	0.37
40	1.16	0.37
45	1.18	0.37
50	1.25	0.37
65	1.42	0.23

To substantiate the heating response of quaternary surfactants, conductivity data was collected at various temperatures for different TBADS concentrations, as shown in Fig. 3. For TBADS concentration of 0.005 M, conductivity increases with the increase in temperature. This observation is in line with that observed in Fig. 1 as well as with the observations in earlier reports.[42] When the conductivity experiments were performed with 0.015 M TBADS, the κ values showed a weak dependence (nearly constant) on temperature. However, the conductivity data for 0.03 M TBADS showed a decrease in κ with temperature. This observation is in sharp contrast to the reported conductivity data for conventional ionic surfactants at higher concentrations.[42] It is difficult to understand the decrease in conductance with temperature for a solution that contains charged species. In a typical solution, conductance generally depends upon mobility, number and ion sizes. The present decrease of κ with temperature (0.03 M TBADS, Fig. 2) can be understood in the light of the following facts: (a) both the counterion (TBA^+) and headgroup will have a certain degree of hydration, which is expected to decrease on heating; (b) this dehydration of the counterion and headgroup causes effective charge neutralization; and (c) due to these abovementioned reasons the charge of the conducting species (counterion and headgroup) may neutralize with a concomitant conversion into nearly non-ionic species. It should be mentioned here that quaternary counterions are less hydrated than inorganic counterions, and the charge of the former can be considered to be buried in a paraffin shell. This may facilitate a quaternary counterion to interact with

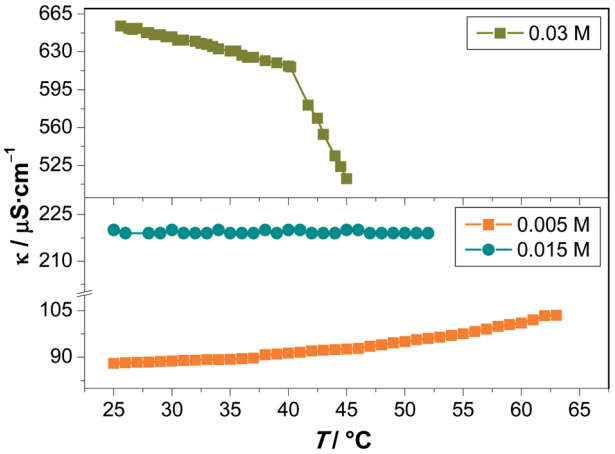

Fig. 3 Variation of specific conductance (κ) *vs.* temperature plot for TBADS at different concentrations.

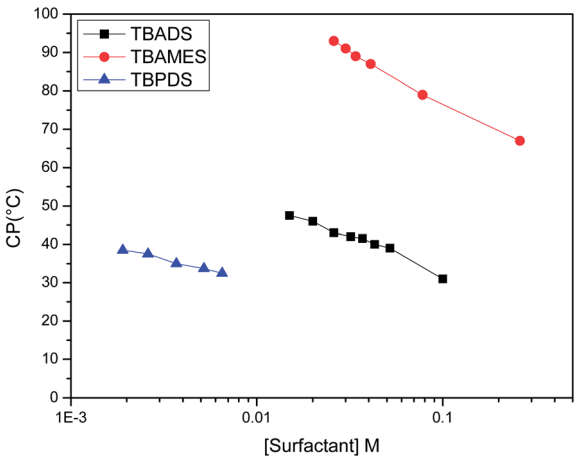

Fig. 4 Variation of cloud point (CP) at different surfactant concentrations.

an anionic micelle electrostatically and hydrophobically. Interestingly, such pseudo-nonionic micelles were proposed to explain the clouding behavior of an ionic surfactant

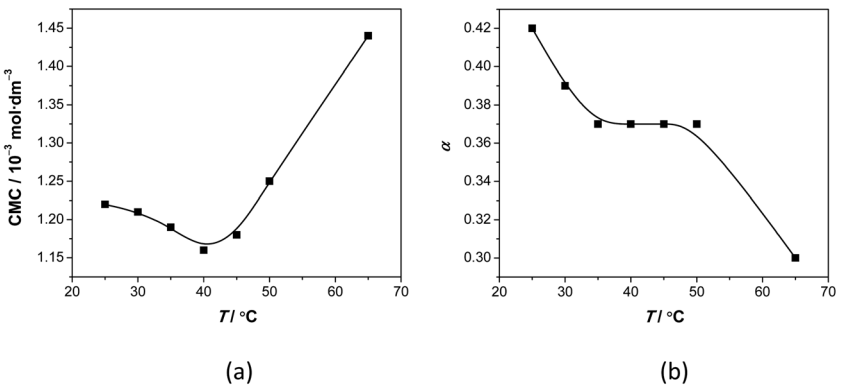

Fig. 2 Temperature effect on (a) cmc and (b) α of TBADS.

system.[5] The above discussion appears sufficient to understand the peculiar behaviour (higher T_m, decrease in α and κ) of quaternary surfactants with respect to temperature.

Clouding phenomenon in anionic surfactant solution

A perusal of the CP data, presented in Fig. 4, indicates that the CP follows the order: TBAMES > TBADS > TBPDS. This order results from various combinations of the counterion and alkyl head group part of the surfactant. Among TBA^+, TBAMES has a higher CP than TBADS. TBAMES shows clouding at a higher temperature due to the presence of one ester group in addition to a sulfonate moiety in its headgroup. The extra ester group may form an H-bond with water molecules due to dipole–dipole interactions, which results in increased hydration and is responsible for the higher CP. The CP for TBPDS is found to be considerably lower than both the TBADS and TBAMES surfactants. This may be due to the nature and bigger size of the TBP^+ counterion, and because of which the surface dehydration is expected to be more. At equal concentrations of TBADS and TBPDS, faster saturation of the micellar surface is expected with TBP^+, and thus more TBP^+ are left to facilitate the approach of various micelles close to each other, resulting in a lower CP.

To get an idea regarding the changes in micelle size with an increase in temperature, DLS studies were performed with various surfactant solutions at different temperatures (below and above the CP). It was observed that two populations of different sizes are present near the CP. This type of behaviour is already reported for other systems,[17,24,44] which indicates that the presence of two types of micelles may be a general feature for ionic surfactants showing clouding. From the lognormal distribution, it was intimated that the effective hydrodynamic diameter of micelles increase considerably near the CP (Fig. 5a). The approach of a grown micelle to other micelles may start, and then at a particular temperature, they lead to the formation of bigger aggregates, which are responsible for the clouding phenomenon. At/after the CP, two phases gradually separate, and one of the two phases now spans the whole scattering volume. This is in consonance with the decrease in size after the CP. The grown micelles participated in linking, forming one phase of bigger aggregates responsible for clouding and the other phase that is left with small sized micelles contribute to scattering, as seen from Fig. 5a. As the micelles grow with increasing temperature, the ratio of the bigger micelles to that of the smaller ones increases with the increasing temperature, which leads to an increase in polydispersity initially. However, after a certain temperature, the micelles are grown and thus the ratio between the two decreases, lowering the polydispersity, which is also an indication of the dominating of one population. Interestingly, the polydispersity of the system reaches a minimum, as phase separation starts. It can be said that only one of the two phases now spans the whole scattering volume, tending the system towards a mono-dispersed phase (Fig. 5b).

Among various studies, NMR spectroscopy has been found to be one of the suitable methods for monitoring the interactions in micellar solutions. Fig. S1–S3 (ESI†) show the chemical structure and ^1H NMR spectra of all the anionic surfactants studied in D_2O. ^1H NMR spectra for all the above mentioned anionic surfactants at variable temperatures (below, at and above CP) were acquired. The cropped ^1H NMR of a representative 0.005 M TBPDS (CP = 27 °C) at variable temperatures shows the shifting of the spectra to a higher δ (ppm) scale as the temperature increases (Fig. 6a). The decrease in the degree of hydration and electron density around N1, a counter ion ($-P-CH_2$) proton, near the micelle surface can easily be ascertained by the chemical shift analysis. The higher δ value corroborates the decrease in hydration and also the onset of attractive interactions between the counterions and the micellar head group. The chemical shifts of the α-methylene protons, which are attached to the sulphate group, are also significantly affected by the charge distribution around it (Fig. S4, ESI†). Therefore, due to the dehydration of the counterion and the surfactant head group, counterion condensation takes place, which may be responsible for the growth of the micelles. This may find support from the fact that the Mitchell–Ninham parameter[45] ($P = v/a_h l$, where v and l are the volume and length of the alkyl part, respectively, and a_h is the head group area of a typical surfactant) increases due to the condensation of various counter ions with a simultaneous decrease in the value of a_h. The increase in P is always reported for the formation of higher order aggregates.[23] The overall micelle charge may also decrease, leading towards a pseudo-nonionic system. To show the effect of the counterion without the interference of other

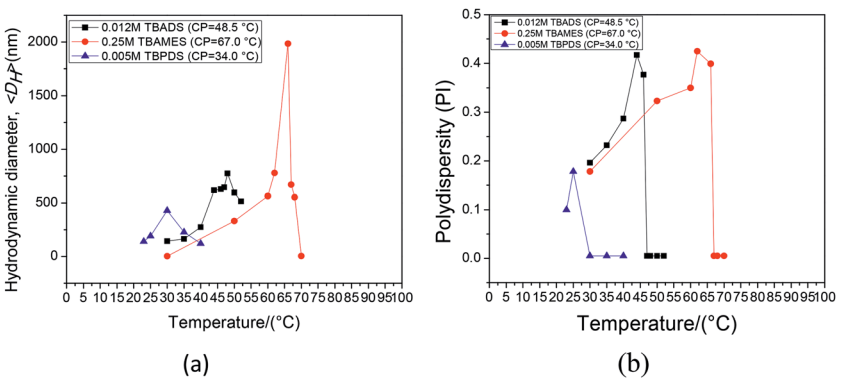

Fig. 5 Temperature effect on (a) hydrodynamic diameter $\langle D_H \rangle$ and (b) polydispersity (PI) of different surfactants solutions.

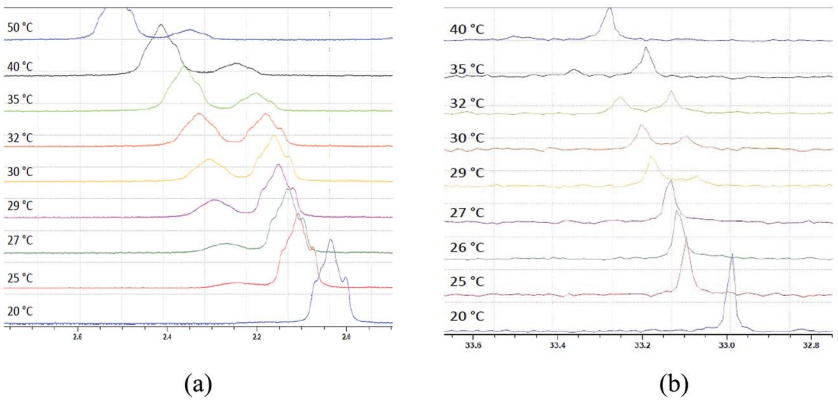

Fig. 6 NMR spectra (a) ^{1}H and (b) ^{31}P for 0.005 M TBPDS at different temperatures below, at and after CP.

neighboring protons, ^{31}P decoupled NMR at different temperatures was also acquired (Fig. 6b). The N1 proton in TBPDS splits into two peaks at higher temperatures. This is due to the alteration of the resultant chemical environment among the two types of micelle population. However, a gradual broadening of the abovementioned peak on heating indicates micelle growth[24,46] as the system approaches the CP. Thus, the broadening and splitting of the peak indicates micelle growth and ultimately the formation of bigger aggregates through the fusion of various micelles *via* dehydrated counter ions at higher temperatures. Similar results are obtained for TBAMES (Fig. S5, ESI†). This study was extended to TX-100, a well known conventional nonionic surfactant that shows clouding on heating wherein no such broadening and splitting of peaks is seen on heating till the CP. This may be due to the presence of more hydrophilic units present in the chain, which on heating may only dehydrate and decrease the polar character of the poly(ethylene glycol) headgroup, giving rise to the attractive interactions responsible for clouding[47] (Fig. S6, ESI†).

To further examine the mechanism taking place during the entire cloud point phenomenon, typical noninvasive 2D NMR studies were carried out for all the anionic surfactants at room temperature (RT) and near the CP. The results of two-dimensional nuclear Overhauser effect spectroscopy (2D NOESY) enabled the identification of the counterion effects with the increase in temperature. A representative 0.03 M TBADS (CP = 42.5 °C) solution is selected here to show the heating effects. On heating, clear cross peaks (absent in 2D COSY, Fig. S7, ESI† and 2D NOESY at RT, Fig. 7a) occur due to the dominating hydrophobic interactions (Fig. 7b). This is due to dehydration at higher temperatures along with the screening electrostatic interactions between the TBA^{+} counter ion and surfactant head group. Strong correlation cross peaks between N1–N4, N1–N3, N1–N2 and S1–N4, S1–N2 protons are seen on approaching the CP, suggesting the intercalation of the counterion butyl chain with increasing temperature. Similar results are seen with 0.005 M TBPDS (CP = 27.0 °C) and 0.25 M TBAMES (CP = 65.0 °C) surfactant solutions (Fig. S8 and S9, ESI†) with the only difference in the signs of the cross peaks in TBAMES near the CP. The signs of the nuclear Overhauser effects (NOE) of all the diagonal and the cross peaks in the TBADS and TBPDS solutions at RT and near the CP are positive, whereas the cross peaks for the TBAMES solution near the CP showed the opposite nature (negative NOE) to that at RT. This means for the TBADS and TBPDS solutions near the CP (lower than the CP for TBAMES), the TBA^{+}/TBP^{+} counterions are not completely dehydrated; thus, the tumbling rate of the intercalated counterion chain in this case is fast, giving a positive

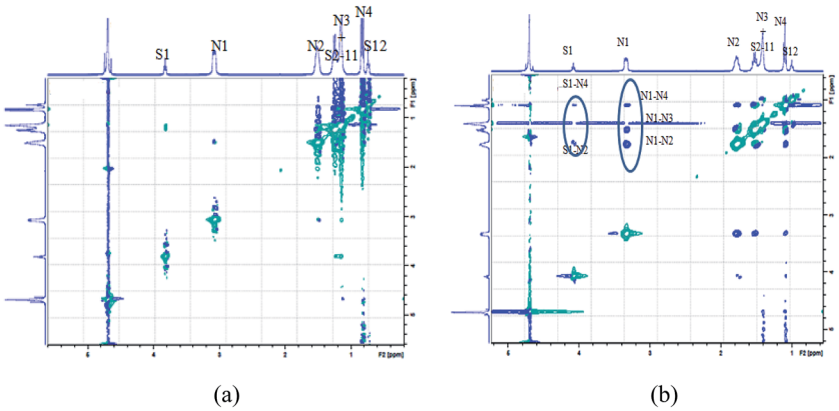

Fig. 7 2D NOESY NMR spectra of 0.03 M TBADS at (a) 18 °C and (b) near the CP.

NOE.[15] For the TBAMES solution near the CP, *i.e.* at 64 °C, the motion of the alkyl part and the TBA^+ counterion is restricted at such high temperature due to the greater insertion of TBA^+ (more dehydrated) into the hydrophobic core. Moreover, the distinct cross peaks, namely, S2–S15 and S2–N4, and more intense peaks, namely, N1–N4, N1–N3 and N1–N2 (Fig. S9, ESI†), are in agreement with the dominating hydrophobic effects. The NOESY results corroborate the proposition that dehydrated TBA^+/TBP^+ ions associate with alkyl heads *via* hydrophobic interactions to form grown micelles at higher temperatures (near the CP). TBA^+/TBP^+ ions first attach to the surface of the anionic micelles and then on further dehydration at higher temperatures get inserted into the hydrophobic core. Though NMR is not directly sensitive to morphological transitions, these transitions can be indirectly assessed from NMR (from the broadening and shifting of peaks) with the knowledge of other techniques.

SANS measurements provide useful information pertaining to the micelle growth and fractional charge for different anionic surfactant solutions in a non-invasive manner. The SANS spectra of 0.0124 M TBADS as a function of temperature before and after the CP are shown in Fig. 8. On increasing the temperature, the cross section decreases remarkably in the low Q region. This is a typical behaviour that was also observed earlier.[24,27] The purpose of the present temperature effect study is to have a sufficiently wide temperature range below and above the CP; therefore, a lower concentration (0.0124 M TBADS; CP = 48.5 °C) was taken. No significant change was observed in the fitted micellar parameters when the solution temperature reaches near the CP (Table T2, ESI†). Once the CP is crossed, the magnitude of the scattering intensity curve starts decreasing in the low Q region. This means the number of individual micelles on heating decrease as the grown micelles fuse *via* the butyl chains of dehydrated TBA^+ and form bigger aggregates. The bigger aggregate sizes are expected to be out of range of the present SANS spectrometer. This phenomenon is actually seen from the decrease in the micellar fraction of individual micelles (which now spans the whole scattering volume) with the increase in temperature after the CP. From earlier studies,[26] it is seen that only 40% of the TBA^+ counterions are adsorbed at the micelle surface due to their bulky nature. Moreover, it was seen that only two butyl chains due to the geometric restrictions can intercalate into the micellar core, and about 75% volume of these tail reside in the core. The intercalation of dehydrated TBA^+/TBP^+ (at higher temperatures near the CP), between the anionic head groups, screen the charge and reduce the electrostatic repulsions between them, and thus the overall charge on the micelle surface decreases (Table T2, ESI†), giving a pseudo nonionic character.

The scattering from the individual micelles exist at and even beyond the CP, suggesting that only a part of the micelles (grown) fuse *via* dehydrated counterions, forming bigger aggregates that are responsible for clouding (Fig. 8). On further increasing the temperature, more micelles grow and participate in the formation of bigger aggregates that are responsible for clouding, resulting in a further decrease of the individual micelle fraction.

To get further insight, the temperature effect was also studied with TBAMES, which gives clouding at a higher temperature and at comparatively higher concentrations than TBADS. The SANS spectra of 0.25 M TBAMES (CP = 65 °C) at various temperatures are shown in Fig. 9. The TBAMES solution behaviour overlaps with both conventional ionic and non-ionic micellar solutions. This behaviour can be understood in the light of the fact that dehydrated TBA^+ counterions associate with ionic micelles to form grown micelles at higher temperatures near the CP and decrease the electrostatic interactions. This is clearly reflected by the lower α values. Table 2 contains the fitted micellar parameters, which show that the length of the semi-major axis (a) increases with temperature from 28.1 to 89.2 Å, and thus confirm the micelle growth on heating. The scattering intensity above the CP is now due to the lower sized anionic micelles, which spans the whole scattering volume in the solution. Here, with the increase in temperature, along with

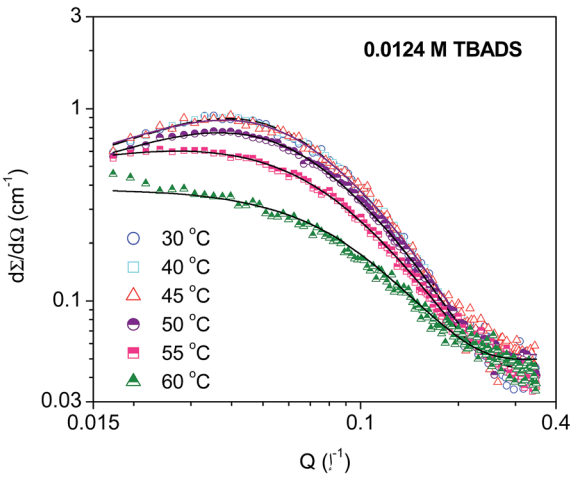

Fig. 8 SANS spectra of 0.0124 M TBADS at varying temperatures below and above the CP.

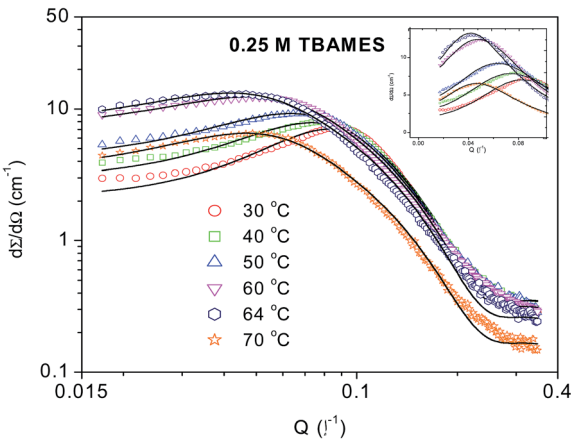

Fig. 9 SANS spectra of 0.25 M TBAMES at different temperatures below and above CP. The inset is a magnification of the low Q data.

Table 2 Fitted micellar parameters of 0.25 M TBAMES at varying temperatures using the prolate ellipsoidal model

Temperature (°C)	Semiminor axis $b = c$ (Å)	Semimajor axis a (Å)	Aggregation number N	Fractional charge α	Micellar fraction (%)
30	16.0	28.1	50	0.06	100
40	16.0	30.5	54	0.06	100
50	16.0	35.6	62	0.05	100
60	16.0	50.7	87	0.04	100
64	16.0	89.2	151	0.03	100
70	16.0	81.8	139	0.01	48

the micelle growth, the onset of attractive interactions is also confirmed from the low Q upturn (inset, Fig. 9). However, in earlier studies,[19,48] micelle disintegration was reported when charged micelles were heated.

The SANS spectra for SDS, which is a typical conventional anionic surfactant (not showing clouding), is shown in Fig. S10 (ESI†). From the fitted micellar parameters of a 0.03 M SDS solution (Table T3, ESI†), it is seen that the ellipsoidal micelle disintegrates (decrease in semi major axis (23 Å to 19.7 Å) on increasing the temperature from 30 °C to 60 °C). TX-100, which is a well known conventional nonionic surfactant that shows clouding on heating, does not show any micelle growth or micellar shape changes that can be reflected in the above-mentioned analysis. This is in consonance with the other results (theoretical as well as experimental) reported for TX-100.[49,50] However, the low Q upturn with increasing temperature due to the attractive interactions is the predominating factor responsible for clouding (Fig. S11 and Table T4, ESI†).

To get further insight, visual evidence regarding the morphological transitions were collected using optical microscopic studies. The typical micrographs for a representative 0.25 M TBAMES surfactant solution are shown in Fig. 10. As evidenced from the micrographs at room temperature (Fig. 10a), the aggregates are very small and their sizes are below the lower detection limit of the polarising microscope. However, near the CP at 64 °C, their sizes are big enough and can now be seen by polarizing optical microscopy (Fig. 10b). Similar observations could be made for other surfactant solutions as well. To obtain clear insight, the two phases at the CP in a 0.1 M TBADS solution were separated and then analysed at RT. It was found that even at RT, the rich phase showed the presence of bigger aggregates (Fig. S12, ESI†), which were seen by POM, unlike that with the lean phase, which again on heating gave even bigger aggregates, as seen in the visible range by a microscope. The grown micelles are clearly seen to be fusing with other micelles, forming bigger aggregates, which are responsible for the clouding phenomenon (Fig. S13, ESI†). This is in agreement with the Langer-Schwartz theory[51] that has the following prediction: the nucleated phase may appear as a cloud of small droplets that grow slowly beyond the critical droplet size or it may be formed as an isolated droplet that rapidly grows to a very large size. The same analogy is drawn for the present surfactant solutions, in which liquid–liquid immiscibility occurs above the lower critical solution temperature (LCST) or CP.

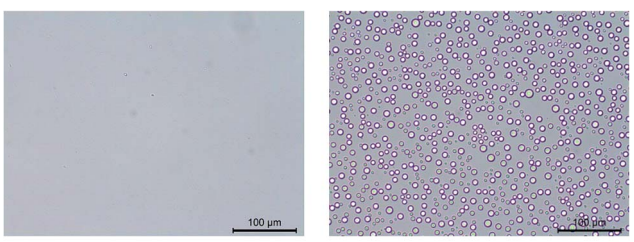

Fig. 10 Optical micrographs for 0.25 M TBAMES at (a) RT and (b) near CP.

Conclusion

This study focuses on several surprising and unexplained features of the temperature dependent self-assembly of anionic surfactants in aqueous solution. The solution behaviour of typical anionic surfactants, the involved morphological transitions (below and above the CP) and the mechanism of clouding are explored by rationalizing observations through experimental evidence along with qualitative arguments using various physicochemical techniques. It is also found that the nature of the counterion and head group part has a predominant role in deciding micellar parameters, solution properties and CP values. An attempt has been made to correlate the structure of ionic surfactants and the clouding phenomenon. The results of DLS, various NMR techniques, SANS and POM are in consonance with the micelle growth facilitated by dehydrated counterions and the surfactant head group. The fusion of these as-grown micelles results in bigger aggregates. Thus, attractive interactions and the formation of bigger aggregates, as confirmed from the NMR and POM results, respectively, are the two key factors involved in the phase separation (clouding) of ionic surfactant solutions. The clouding in anionic surfactants in general and at low mole fractions (x) with TBP^+ surfactants especially may find use in CPE systems for various charged species as well as thermally labile compounds, such as vitamins and thermo-responsive drugs/proteins, under ambient conditions.

Acknowledgements

The authors are thankful to UGC-DAE CSR, (CRS-151) Mumbai Centre, India and CSIR, New Delhi, India (Sanction no.: 09/114/(0191)/2013-EMR-I) for the financial support.

References

1 D. Chandler, *Nature*, 2005, **437**, 640–647.
2 S. Peleshanko, K. D. Anderson, M. Goodman, M. D. Determan, S. K. Mallapragada and V. T. Tsukruk, *Langmuir*, 2007, **23**, 25–30.
3 D. J. Mitchell, G. J. T. Tiddy, L. Waring, T. Bostock and M. P. McDonald, *J. Chem. Soc., Faraday Trans. 1*, 1983, **79**, 975–1000.
4 K. H. Gabor, C. Naomi and V. W. Ray, *Langmuir*, 1996, **12**, 916–920.
5 S. R. Raghavan, H. Edlund and E. W. Kaler, *Langmuir*, 2002, **18**, 1056–1064.
6 G. G. Waar, T. N. Zemb and M. Drifford, *J. Phys. Chem.*, 1990, **94**, 3086–3092.
7 S. A. Buckingham, C. J. Garvery and G. G. Waar, *J. Phys. Chem.*, 1993, **97**, 10236–10244.
8 B. L. Bales and R. Zana, *Langmuir*, 2004, **20**, 1579–1581.
9 J. X. Xiao and G. X. Zhao, *Chin. J. Chem.*, 1994, **12**, 552–554.
10 P. Mukherjee, S. K. Padhan, S. Dash, S. Patel and B. K. Mishra, *Adv. Colloid Interface Sci.*, 2011, **162**, 59–79.
11 S. Kumar and A. Bhadoria, *J. Chem. Eng. Data*, 2012, **57**, 521–525.
12 M. Benrraou, B. L. Bales and R. Zana, *J. Phys. Chem. B*, 2003, **107**, 13432–13440.
13 B. L. Bales, M. Benrraou, K. Tiguida and R. Zana, *J. Phys. Chem. B*, 2005, **109**, 7987–7997.
14 T. Ahmad, S. Kumar, Z. A. Khan and Kabir-ud-Din, *Colloids Surf., A*, 2007, **294**, 130–136.
15 J. H. Lin, W. S. Chen and S. S. Hou, *J. Phys. Chem. B*, 2013, **117**, 12076–12085.
16 U. Thapa, J. Dey, S. Kumar, P. A. Hassan, V. K. Aswal and K. Ismail, *Soft Matter*, 2013, **9**, 11225–11232.
17 Y. Haiqing, Z. Zukang, H. Jianbin, Z. Rong and Z. Yongyi, *Angew. Chem., Int. Ed.*, 2003, **42**, 2188–2191.
18 P. R. Majhi and A. Blume, *J. Phys. Chem. B*, 2002, **106**, 10753–10763.
19 V. Yu, S. Bezzobotnov, L. Borbebly, B. Cser, I. A. Farago, Y. Gladkih, M. Ostanevich and S. Vassi, *J. Phys. Chem.*, 1988, **92**, 5138–5143.
20 S. Forster and T. Plantenberg, *Angew. Chem.*, 2002, **114**, 712–739.
21 J. Narayanan, E. Mendes and C. Manohar, *Int. J. Mod. Phys. B*, 2002, **16**, 375–382.
22 S. J. Ryhanen, V. M. J. Saily, M. J. Parry, P. Luciani, G. Mancini, J. M. I. Alakoskela and P. K. J. Kinnunen, *J. Am. Chem. Soc.*, 2006, **128**, 8659–8663.
23 S. D. Tanner, A. M. Ketner and S. R. Raghavan, *J. Am. Chem. Soc.*, 2006, **128**, 6669–6675.
24 S. Kumar, A. Bhadoria, H. Patel and V. K. Aswal, *J. Phys. Chem. B*, 2012, **116**, 3699–3703.
25 R. Zana, M. Benrraou and B. L. Bales, *J. Phys. Chem. B*, 2004, **108**, 18195–18203.
26 V. K. Aswal and J. Kohlbrecher, *Chem. Phys. Lett.*, 2006, **424**, 91–96.
27 Kabir-ud-Din, D. Sharma, Z. A. Khan, V. K. Aswal and S. Kumar, *J. Colloid Interface Sci.*, 2006, **302**, 315–321.
28 A. Zilman, S. A. Safran, T. Sottmann and R. Strey, *Langmuir*, 2004, **20**, 2199–2207.
29 T. J. Drye and M. E. Cates, *J. Chem. Phys.*, 1992, **96**, 1367.
30 P. Panizza, G. Cristobal and J. Curely, *J. Phys.: Condens. Matter*, 1998, **10**, 11659.
31 H. Bock and K. E. Gubbins, *Phys. Rev. Lett.*, 2004, **92**, 135701–135704.
32 P. Yan, J. Huang, R. C. Lu, C. Jin, J. X. Xiao and Y. M. Chen, *J. Phys. Chem. B*, 2005, **109**, 5237–5242.
33 G. C. Kalur and S. R. Raghavan, *J. Phys. Chem. B*, 2005, **109**, 8599–8604.
34 Y. Yan, L. Li and H. Hofffmann, *J. Phys. Chem. B*, 2006, **110**, 1949–1954.
35 Y. Sato, M. N. Shin-ichiro and K. Yoshikawa, *Chem. Phys. Lett.*, 2003, **380**, 279–285.
36 V. K. Aswal and P. S. Goyal, *Curr. Sci.*, 2000, **79**, 947–953.
37 J. B. Hayter and J. Penfold, *J. Colloid Interface Sci.*, 1983, **261**, 1022–1030.
38 S. H. Chen and T. L. Lin, in *Methods of Experimental Physics*, ed. D. L. Price and K. Skold, Academic Press, New York, 1987; vol. 23, p. 489.
39 S. Kumar, N. Parveen and Kabir-ud-Din, *J. Phys. Chem. B*, 2004, **108**, 9588–9592.
40 S. Kumar and K. Parikh, *J. Surfactants Deterg.*, 2013, **16**, 739–749.
41 L. J. Chen, S. Y. Lin and C. C. Huang, *J. Phys. Chem. B*, 1998, **102**, 4350–4356.
42 C. V. Giongo and B. L. Bales, *J. Phys. Chem. B*, 2003, **107**, 5398–5403.
43 B. W. Barry and R. Wilson, *Colloid Polym. Sci.*, 1978, **256**, 251.
44 D. K. Rout, S. Chauhan and A. Agarwal, *Ind. Eng. Chem. Res.*, 2009, **48**, 8842–8847.
45 J. N. Israelachvili, D. J. Mitchell and B. W. Ninham, *J. Chem. Soc., Faraday Trans. 2*, 1976, **72**, 1525–1568.
46 M. Villeneuve, R. Ootsu, M. Ishiwata and H. Nakahara, *J. Phys. Chem. B*, 2006, **110**, 17830–17839.
47 G. Karlstrom, *J. Phys. Chem.*, 1985, **89**, 4962–4964.
48 S. Kumar, V. K. Aswal, A. Z. Naqvi, P. S. Goyal and Kabir-ud-Din, *Langmuir*, 2001, **17**, 2549–2551.
49 R. J. Robson and E. A. Dennis, *J. Phys. Chem.*, 1977, **81**, 1075–1078.
50 A. B. Mandai, S. Ray, A. M. Biswas and S. P. Mouiik, *J. Phys. Chem.*, 1980, **84**, 856–859.
51 S. Langer and A. J. Schwartz, *Phys. Rev. A*, 1980, **21**, 948–958.

